Supplementary materials for

Mathematical modeling of human oocyte aneuploidy

Katarzyna M Tyc, Rajiv C McCoy, Karen Schindler, Jinchuan Xing

This PDF file includes:

Fig. S1, S2, S3, S4, S5, S6, S7

Tables S1, S2, S3

Supplementary Figures

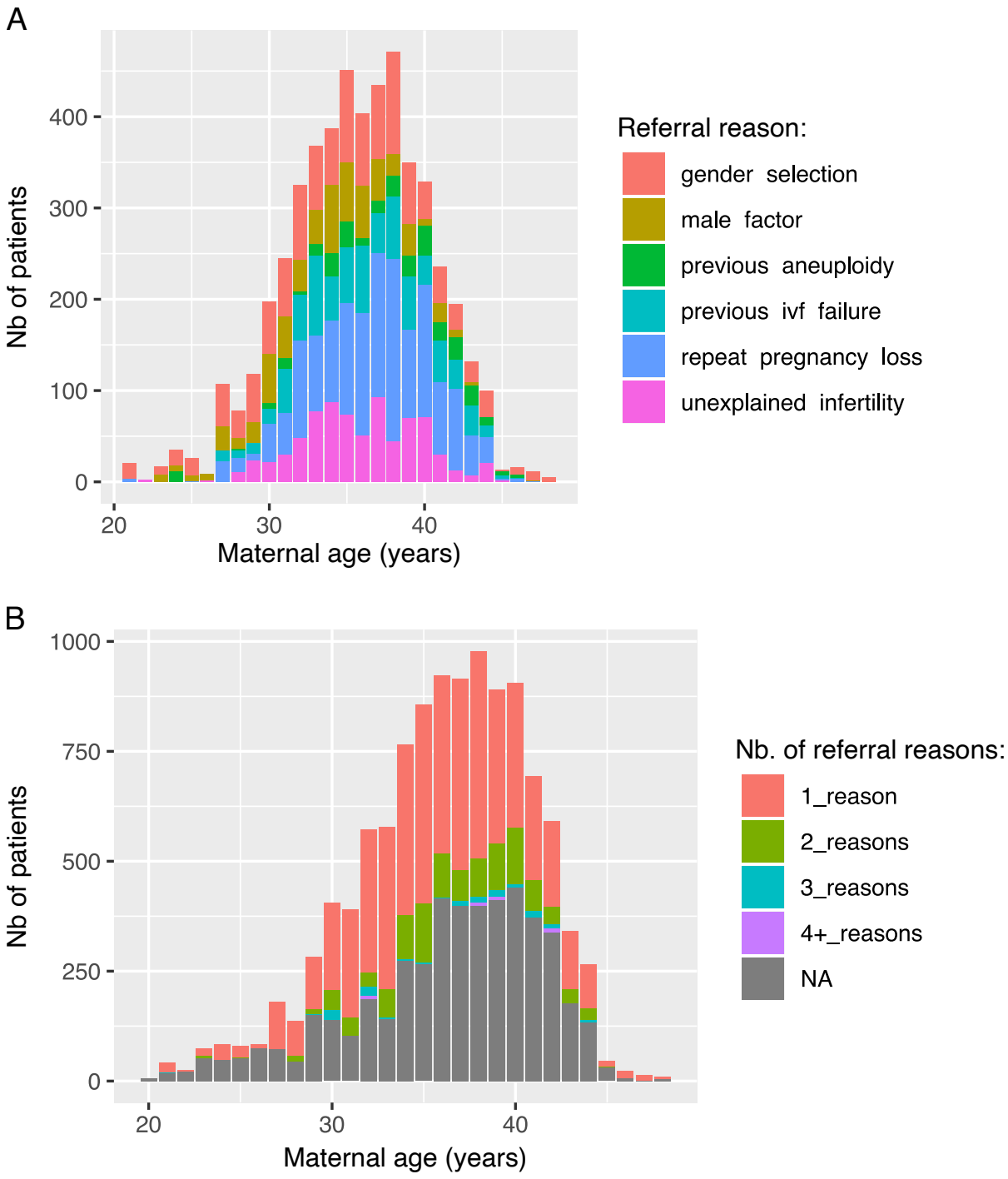

Figure S1. Clinical histories among the analyzed patients stratified by the maternal age. No clear association emerges for either single referral reason (A) or double (B), indicating that referral reasons likely do not act as potential confounding factors of the analysis and/or modeling results. Many of the patients had no recorded referral reason (B, grey bar). Patients with clinical history "translocation" or "advanced_maternal_age" were not considered in the analysis.

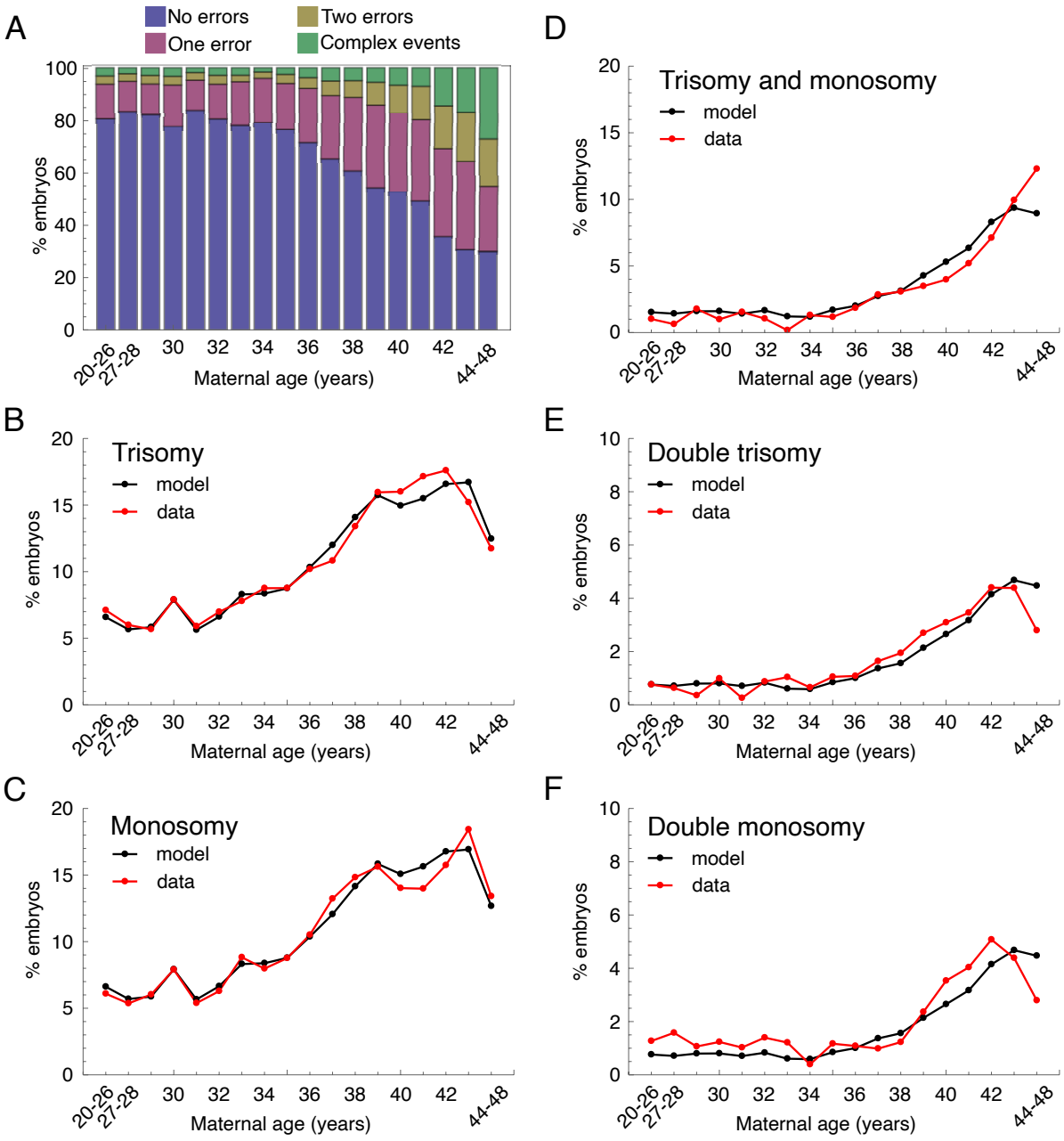

Figure S2. Assessment of model agreement with the data. (A) Karyotype counts extracted from day-5 PGT-A data. 'No error' category (blue bars) represents the proportion of euploid embryos in the dataset. 'One error' category (red bars) represents the proportion of embryos with reported single monosomy or single trisomy. 'Two errors' category (yellow bars) represents the proportion of embryos with two aneuploid chromosomes. 'Complex events' (green bars) accounts for embryos with all the remaining karyotypes. **(B-F)** Detailed view on the 'One error' (red bars in A and Fig. 2B) and the 'Two errors' (yellow bars in A and Fig. 2B). Plotted are data and model simulations for single trisomy (B), single monosomy (C), both trisomy and monosomy (D), two trisomic chromosomes (E), and two monosomic chromosomes (F). All observations are shown in red and all model simulations in black.

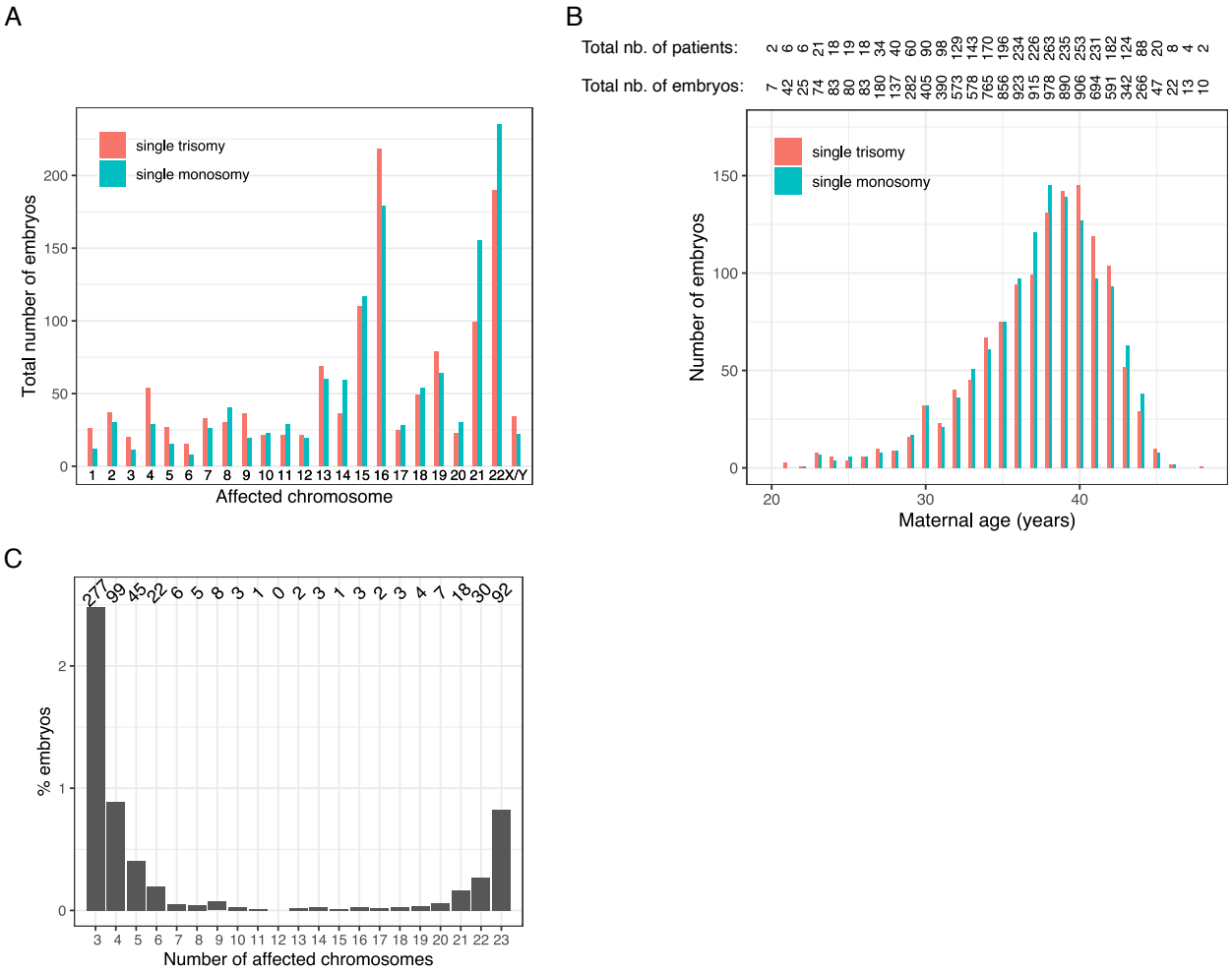

Figure S3. Single error and complex cases analysis. (A-B) Single errors were stratified by (A) chromosome, or (B) maternal age. Total number of patients and embryos evaluated for aneuploidy status in each age category are indicated above the panel B. In this dataset, the incidence of single trisomies and single monosomies are similar across all chromosomes (A). In line with previous reports (e.g., (41), (43) in the main text), single aneuploidies involving chromosomes 15, 16, 21, and 22 are most enriched. (B) Maternal age was not significantly associated with the trisomy:monosmy ratio. **(C)** Embryos with complex karyotypes (i.e., three or more chromosome errors) were stratified by the number of chromosomes affected, from 3 to 23 (22 autosomes and the sex chromosome X/Y) (x-axis) and expressed as percent of all embryos (y-axis). The number of embryos in each category is labelled on the top of the bar.

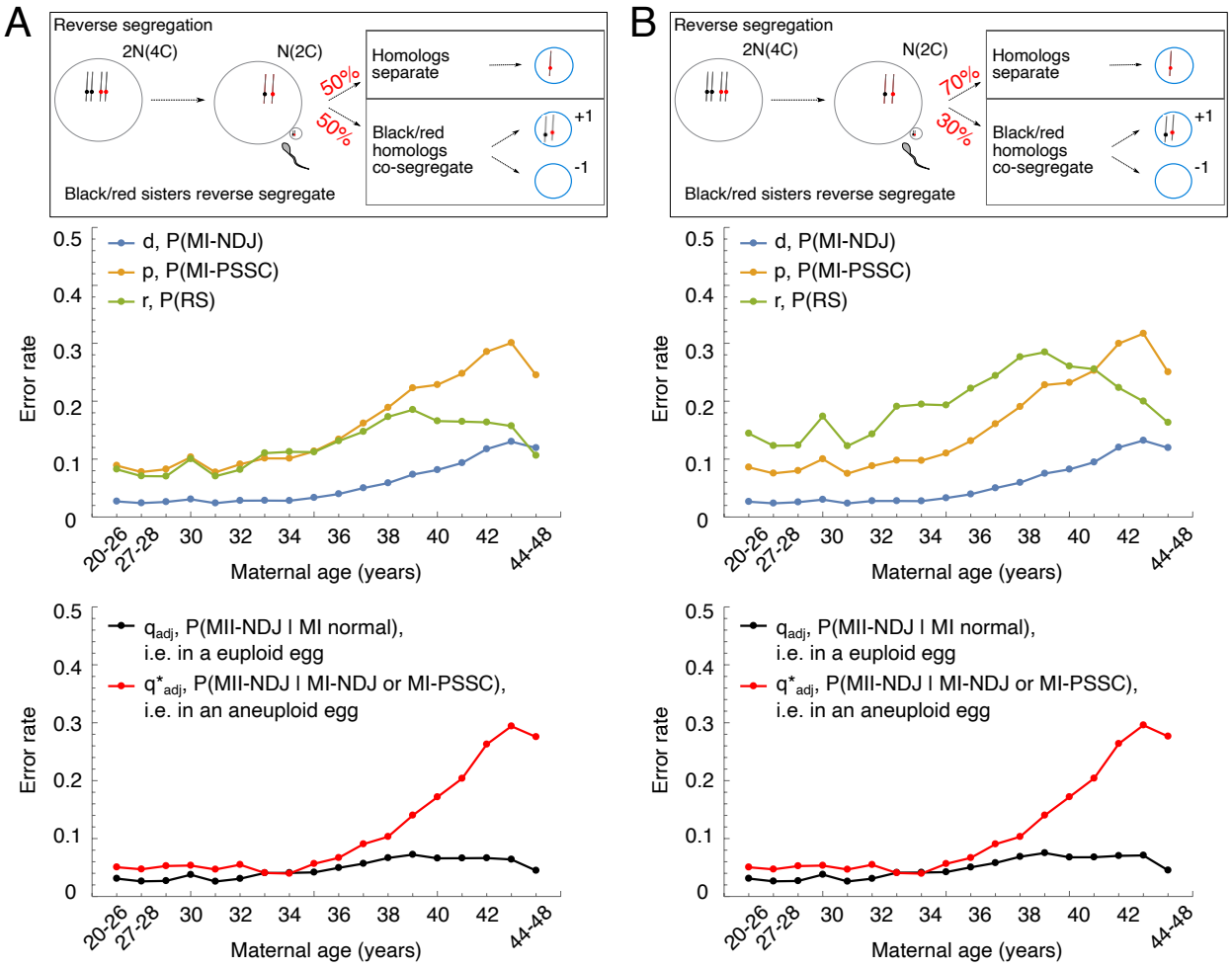

Figure S4. Effect of RS on model parameter estimates. In the boxed areas, C indicates the number of chromatids in a haploid gamete (N). For zygotic maternal pronuclei (blue circles), only a deviation from normal haploid status [i.e., N(1C)] is noted. **(A)** In younger patient cohort (<38y) and in the absence of meiotic drive, incidence of RS is estimated to approximate closely MI-PSSC rates. The indicated drop in RS for older patients is due to the increase of double-error and complex karyotypes in this patient cohort. RS affecting multiple chromosomes is accounted by the complex cases category. **(B)** If meiotic drive holds, then RS is estimated to be more common than MI-PSSC. Again, in older patients the RS rate drops due to the increase of double-errors and complex karyotypes. MII error rates remain largely unaffected by the strength of the meiotic drive acting upon RS.

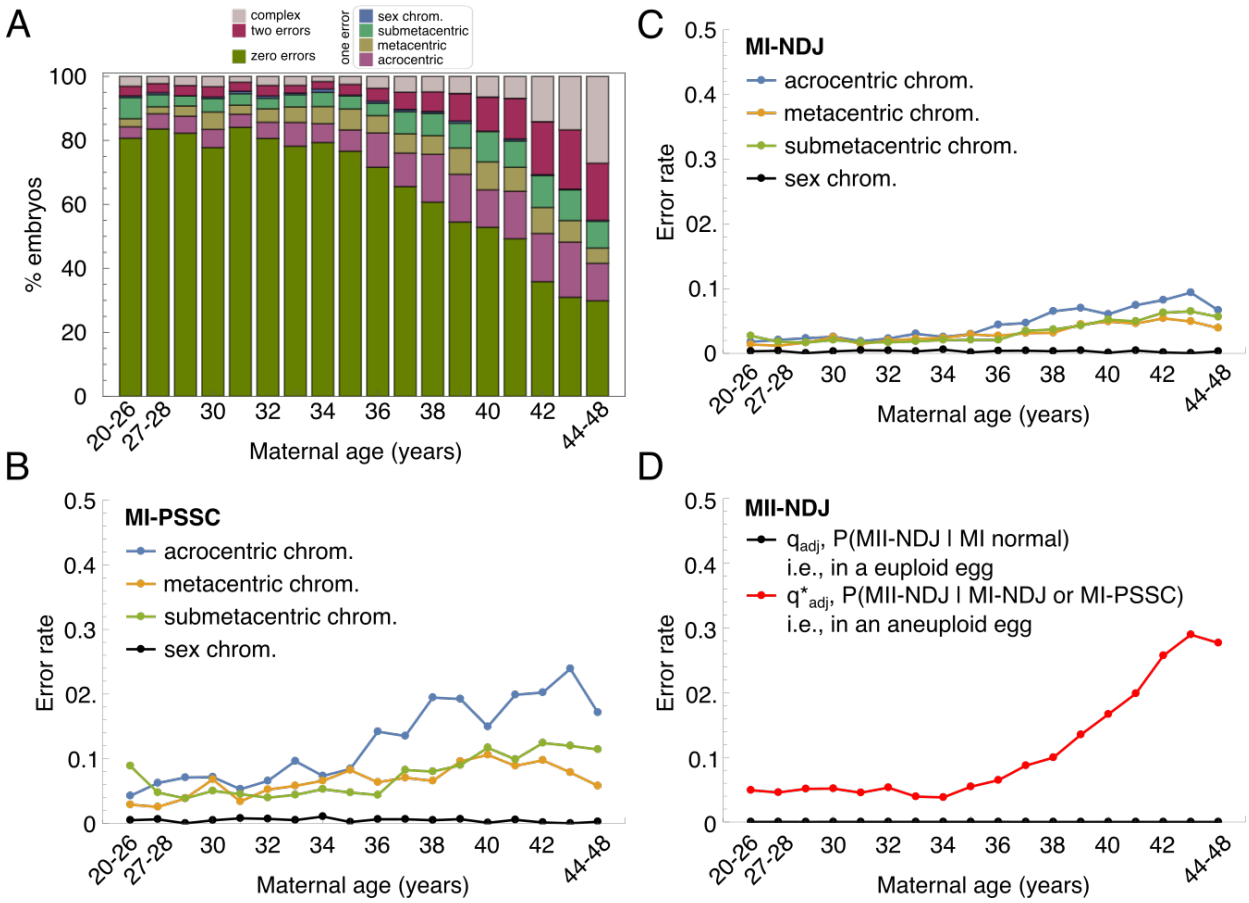

Figure S5. Chromosome type-specific estimates of meiosis I errors. (A) Single aneuploidies for acrocentric (chromosomes 13, 14, 15, 21, 22), metacentric (chromosomes 1, 3, 16, 19, 20), submetacentric (chromosomes 2, 4 to 12, 17, 18) and sex chromosomes (chromosomes X and Y) were grouped together (as indicated by the color legend). Proportion of embryos with zero errors is represented with green bars, embryos with two errors are shown with dark red bars and complex categories with light brown. **(B-C)** Meiosis error rates were estimated for each chromosome group (either for acrocentric, metacentric, submetacentric or sex chromosomes), leading to (B) four MI-PSSC and (C) four MI-NDJ rates, in total. **(D)** Estimated values for MII-NDJ error rates either in euploid (black lines) or aneuploid eggs (red lines). Adjusted MII-NDJ error rates are plotted (see Methods in main text for details).

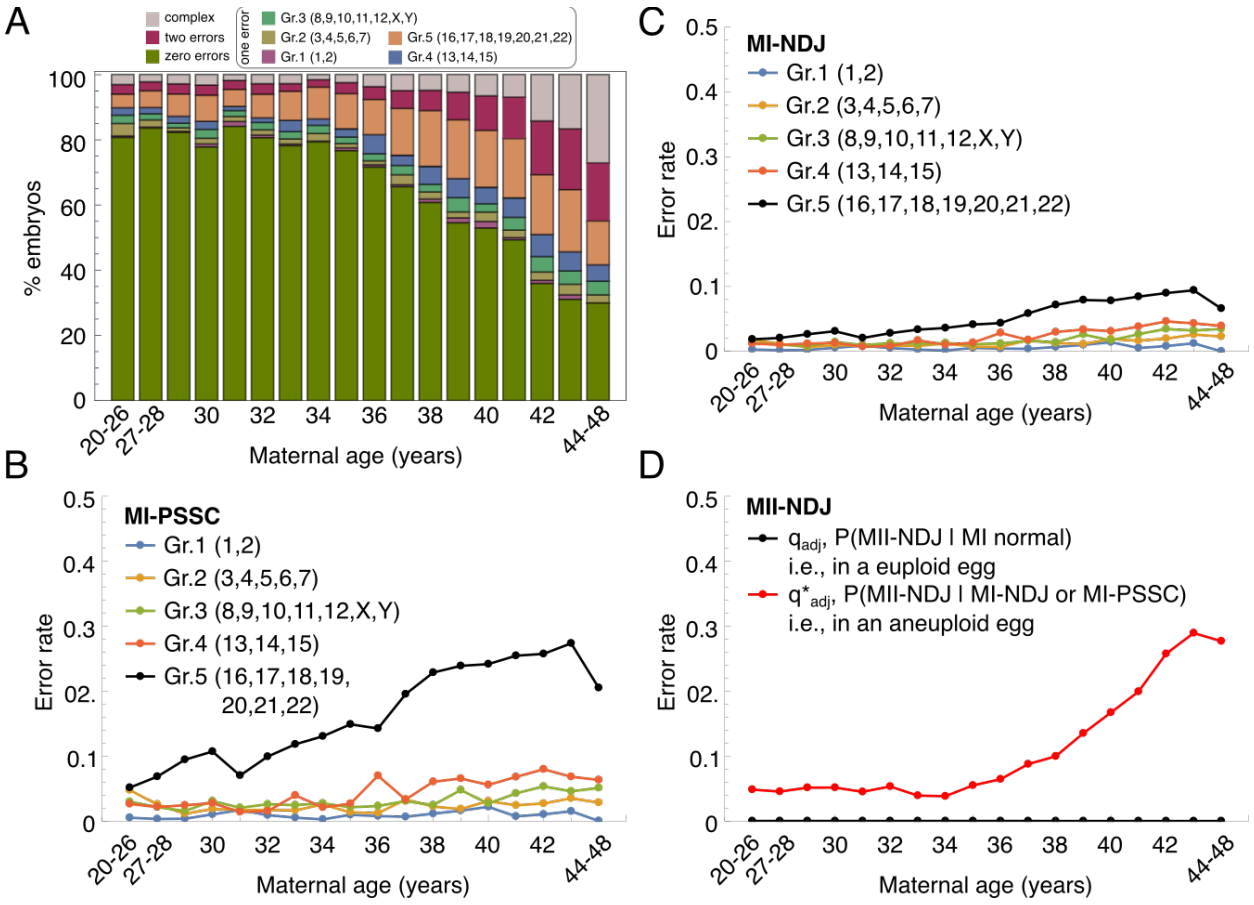

Figure S6. Chromosome size-specific estimates of meiosis I errors. (A) Single aneuploidies for largest to smallest chromosomes, as indicated in the figure legend. Proportion of embryos with zero errors is represented with green bars, embryos with two errors are shown with dark red bars and complex categories with light brown. **(B-C)** Meiosis error rates were estimated for each chromosome group (Gr. 1 to 5), leading to (B) five MI-PSSC and (C) five MI-NDJ rates, in total. **(D)** Estimated values for MII-NDJ error rates either in euploid (black lines) or aneuploid eggs (red lines). Adjusted MII-NDJ error rates are plotted (see Methods in main text for details).

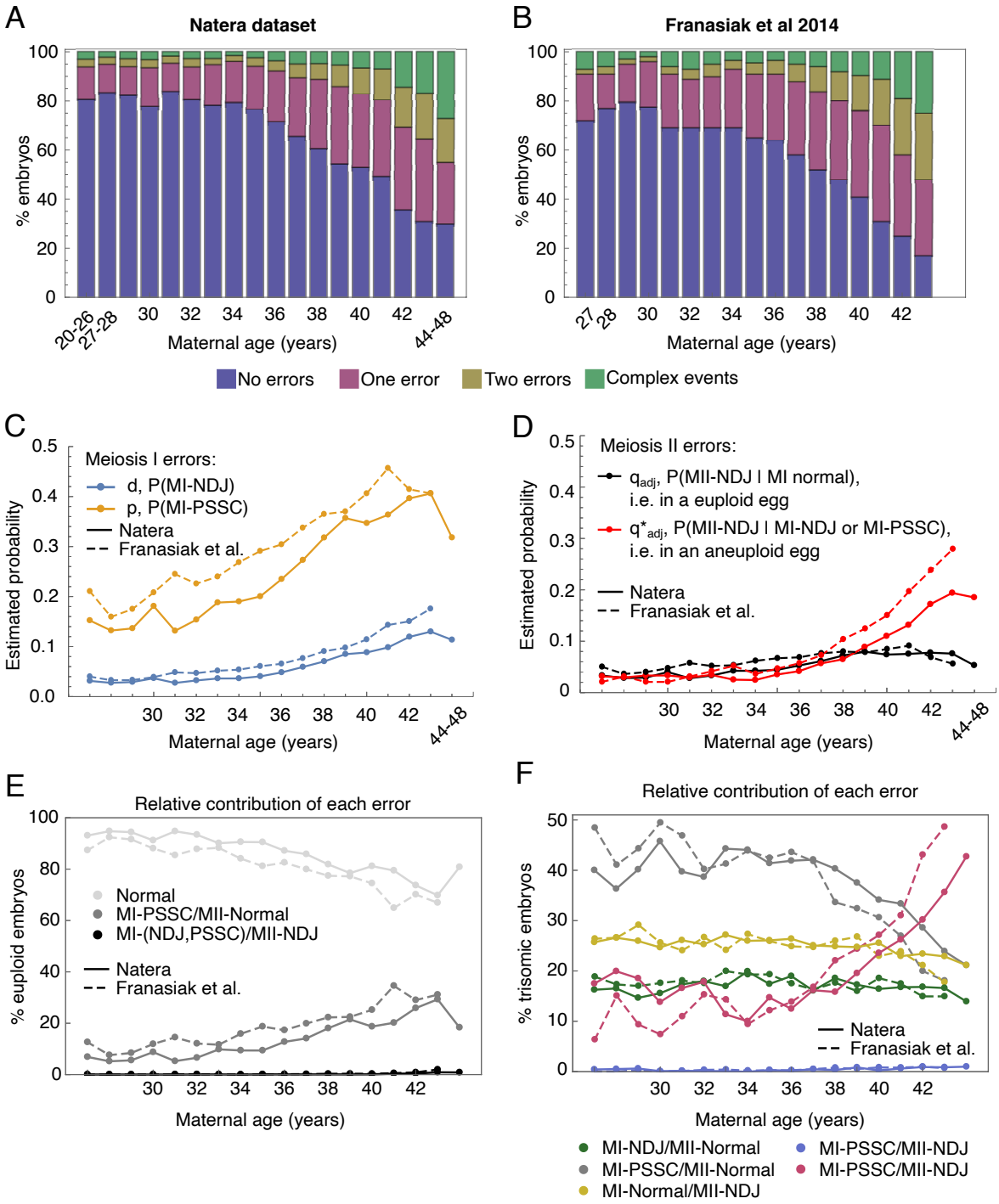

Figure S7. Datasets and model estimates. (A) A copy of Fig. S2A plotted here for ease of comparison. **(B)** Karyotype counts for selected ages extracted from Fig. 3A as published in Franasiak et al 2014. 'No error' category (blue bars) represents the proportion of euploid embryos in the dataset. 'One error' category (red bars) represents the proportion of embryos with single monosomy or single trisomy. 'Two errors' category (yellow bars) represents the proportion of embryos with two aneuploid chromosomes. 'Complex events' (green bars) accounts for embryos with all the remaining karyotypes. **(C-D)** Estimated error rates in each age

category based on either of the two datasets indicated. In (C)**,** the MI-PSSC error rate (*p*) and MI-NDJ error rate (*d*) are shown. In (D), the adjusted MII-NDJ error rate in a euploid egg (*q*) or in an aneuploid egg (*q**) are shown. Adjusted MII rates are used to account for the MI outcome (see Methods). See indication on the figure, to determine which dataset was used for each estimate shown. **(E-F)** Model simulation results based on parameter estimates derived from the two datasets. Karyotypes and underlying error mechanisms were stratified by maternal age categories. **(E)** Relative contribution of meiotic errors to euploid embryo source. Light grey represents a proportion of euploid embryos obtained from normal meiosis, MI-Normal/MII-Normal. Dark grey indicates a proportion of euploid embryos as a result of MI-PSSC/MII-Normal. In black indicated are proportions of euploid embryos from MI-NDJ/MII-NDJ and MI-PSCC/MII-NDJ. **(F)** Relative contribution of meiotic errors to single trisomy embryo source. Green and grey represent proportions of trisomic embryos as an outcome of MI-NDJ/MII-Normal and MI-PSSC/MII-Normal, respectively. In yellow marked are outcomes of MI-Normal/MII-NDJ. In blue and red marked are outcomes of MI-PSSC/MII-NDJ on the same chromosome (depicted in red in Fig. 1) and a different one (depicted in blue in Fig. 1), respectively.

Supplementary Tables

Table S1. Parameter estimations results for each of the model variants tested using embryo counts. 'Model 2 with RS' was tested with the meiotic drive with 77% vs 23% (see Fig. 1).

	d	p	r	c	q	q*	$q^{\#}$	q_{adj} = (1-d-p-r-c)*23*q	q^{*}_{adj} = 45*0.5*q^{*}*(d+p)
Model 1	0	0.293	-	0.072	0.007	-	-	-	-
Model 2	0.059	0.279	-	0.057	0.004	0.016	-	0.056	0.121
Model 3	0.003	0.377	-	0.057	0.003	$4.5x10^{-5}$	0.016	-	-
Model 2 with RS	0.05	0.051	0.835	0.057	0.034	0.041	-	0.005	0.093

Table S2. Age-specific parameter estimation results for Model 2 and embryo counts.

age	d	p	c	q	q*
<27	0.031	0.152	0.030	0.002	0.013
27-28	0.027	0.132	0.022	0.002	0.014
29	0.029	0.136	0.028	0.002	0.015
30	0.037	0.181	0.032	0.002	0.011
31	0.027	0.131	0.018	0.001	0.014
32	0.032	0.154	0.028	0.002	0.014
33	0.036	0.188	0.028	0.002	0.008
34	0.036	0.190	0.016	0.002	0.008
35	0.040	0.200	0.025	0.003	0.011
36	0.048	0.235	0.037	0.003	0.011
37	0.059	0.273	0.049	0.004	0.013
38	0.070	0.318	0.048	0.006	0.012
39	0.085	0.357	0.054	0.007	0.015
40	0.088	0.347	0.065	0.006	0.018
41	0.098	0.363	0.069	0.007	0.021
42	0.119	0.396	0.142	0.010	0.024
43	0.130	0.406	0.167	0.011	0.026
>43	0.113	0.318	0.271	0.008	0.030

Table S3. Age-specific parameter estimation results for Model 2, based on data extrapolated from Franasiak et al 2014, Fig 3A.

age	d	p	c	q	q*
27	0.040	0.211	0.070	0.003	0.006
28	0.033	0.159	0.060	0.002	0.012
29	0.033	0.175	0.030	0.002	0.008
30	0.039	0.208	0.020	0.003	0.006
31	0.048	0.245	0.060	0.004	0.008
32	0.047	0.226	0.070	0.003	0.011
33	0.052	0.240	0.050	0.004	0.013
34	0.054	0.268	0.035	0.004	0.008

35	0.061	0.291	0.045	0.005	0.010
36	0.066	0.304	0.035	0.005	0.011
37	0.077	0.337	0.050	0.006	0.013
38	0.091	0.365	0.060	0.007	0.017
39	0.098	0.370	0.080	0.008	0.019
40	0.114	0.406	0.095	0.010	0.021
41	0.143	0.457	0.110	0.014	0.023
42	0.150	0.414	0.190	0.012	0.029
43	0.176	0.406	0.250	0.015	0.032